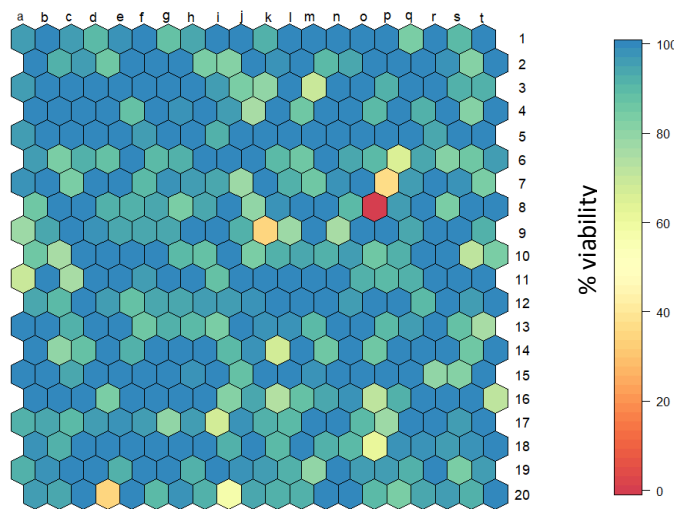


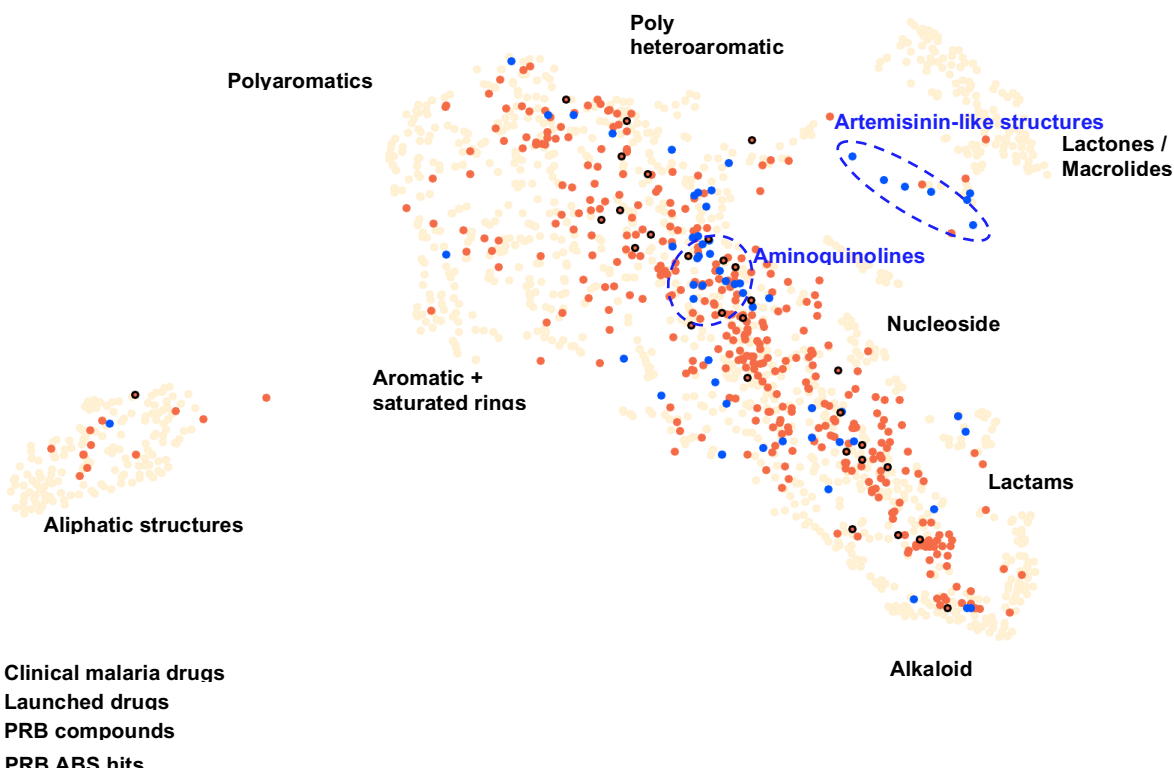
## SUPPLEMENTARY INFORMATION

### Multistage and transmission-blocking targeted antimalarials discovered from the open-source MMV Pandemic Response Box

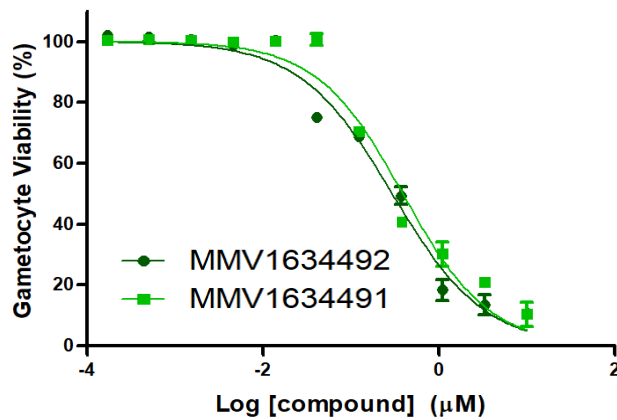
Janette Reader<sup>1a</sup>, Mariëtte E. van der Watt<sup>1a</sup>, Dale Taylor<sup>2</sup>, Claire Le Manach<sup>2</sup>, Nimisha Mittal<sup>3</sup>, Sabine Ottile<sup>3</sup>, Anjo Theron<sup>4</sup>, Phanankosi Moyo<sup>1</sup>, Erica Erlank<sup>5</sup>, Luisa Nardini<sup>5</sup>, Nelius Venter<sup>5</sup>, Sonja Lauterbach<sup>6</sup>, Belinda Bezuidenhout<sup>6</sup>, Andre Horatscheck<sup>2</sup>, Ashleigh van Heerden<sup>1</sup>, Natalie J. Spillman<sup>7</sup>, Anne N. Cowell<sup>3</sup>, Jessica Connacher<sup>1</sup>, Daniel Opperman<sup>1</sup>, Lindsey M. Orchard<sup>8</sup>, Manuel Llinás<sup>8, 9</sup>, Eva S. Istvan<sup>7</sup>, Daniel E. Goldberg<sup>7</sup>, Grant A. Boyle<sup>2</sup>, David Calvo<sup>10</sup>, Dalu Mancama<sup>4</sup>, Theresa L. Coetzer<sup>6</sup>, Elizabeth A. Winzeler<sup>3</sup>, James Duffy<sup>11</sup>, Lizette L. Koekemoer<sup>5</sup>, Gregory Basarab<sup>2</sup>, Kelly Chibale<sup>2,12</sup>, Lyn-Marié Birkholtz<sup>1\*</sup>



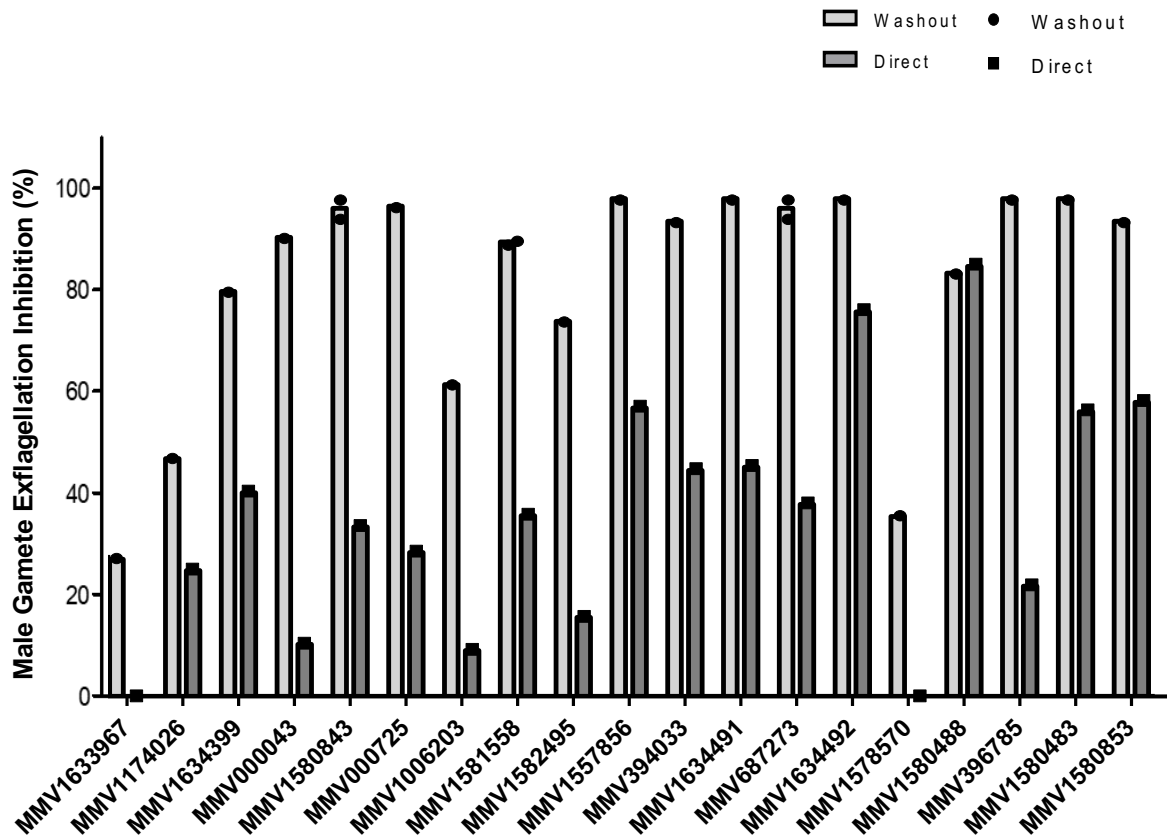
**Supplementary Fig. 1:** Supra-hexoplot for % viability of CHO cells after treatment with compounds at 2  $\mu$ M. Figure supplementary to Figure 2A. Compound identities, placement and individual values are provided in supplementary File S1.



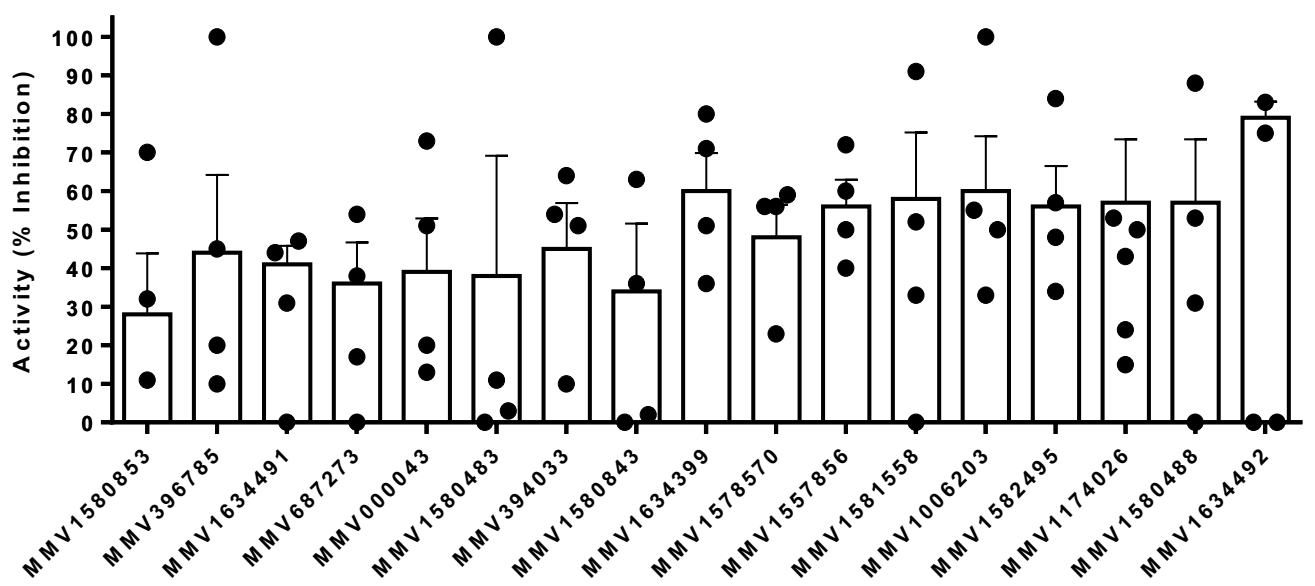
**Supplementary Fig. 2:** Structural diversity of the MMV PRB compared to Malaria Clinical Drugs. MMV PRB (red dots) and Malaria Clinical Drugs (blue dots) chemical spaces are plotted in the Launched Drugs Space (beige dots). The Launched Drug Space is available as standard dataset within the StarDrop V 6.6 software. Supplementary figure to Figure 4.



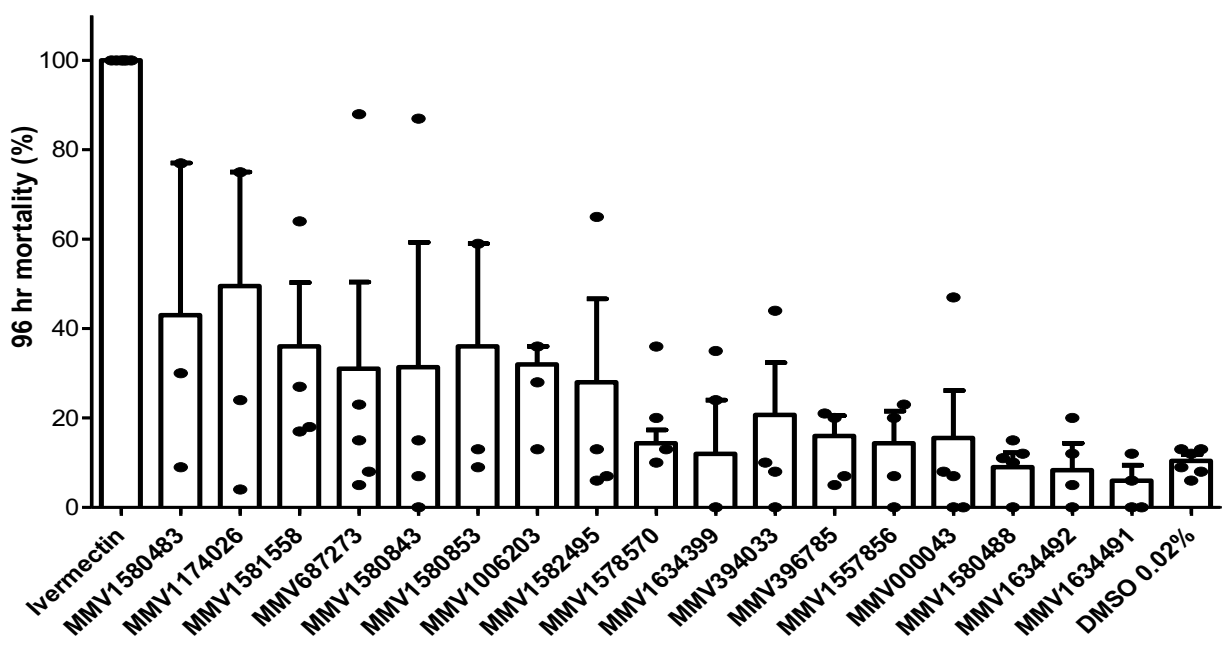
**Supplementary Fig. 3:** Gametocyte-specific compounds were enriched for azole antifungals, including MMV1634491 and MMV1634492, with dose-responses of these two compounds indicated after 48 h exposure to stage IV/V gametocytes and evaluated on the PrestoBlue® assay. Data are from three independent biological repeats ( $n=3$ ), each performed in technical triplicates, mean  $\pm$  S.E. Supplementary figure to Fig 5.



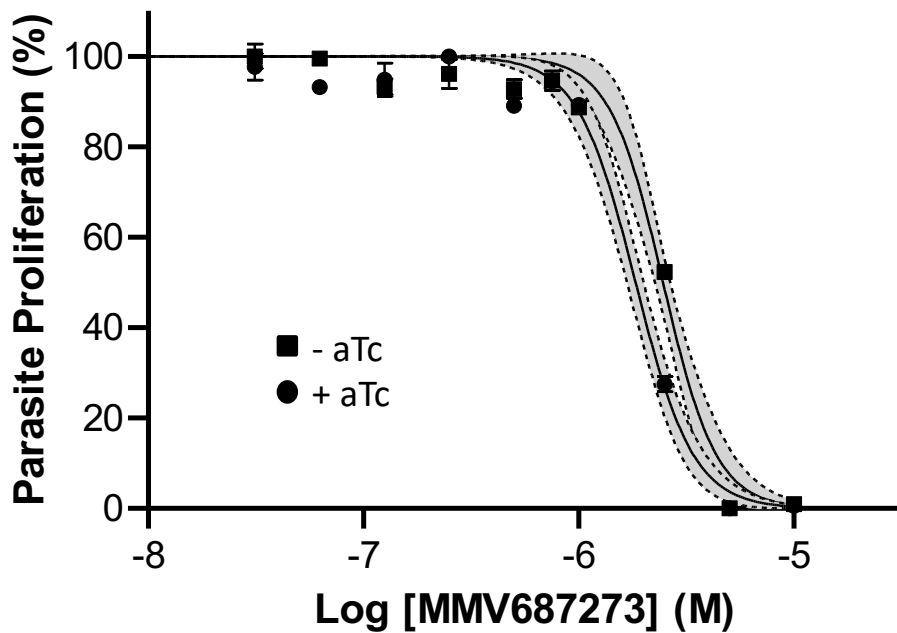
**Supplementary Fig. 4:** Inhibition of male gamete exflagellation in both direct or washout format. Figure supplementary to Figure 5B. Direct: compound added during induction of male exflagellation (30 min incubation), washout: stage V gametocytes treated with compound for 48 h, compound washed out and male gamete exflagellation tested in absence of compounds. Data are from duplicate experiments  $\pm$  S.D.



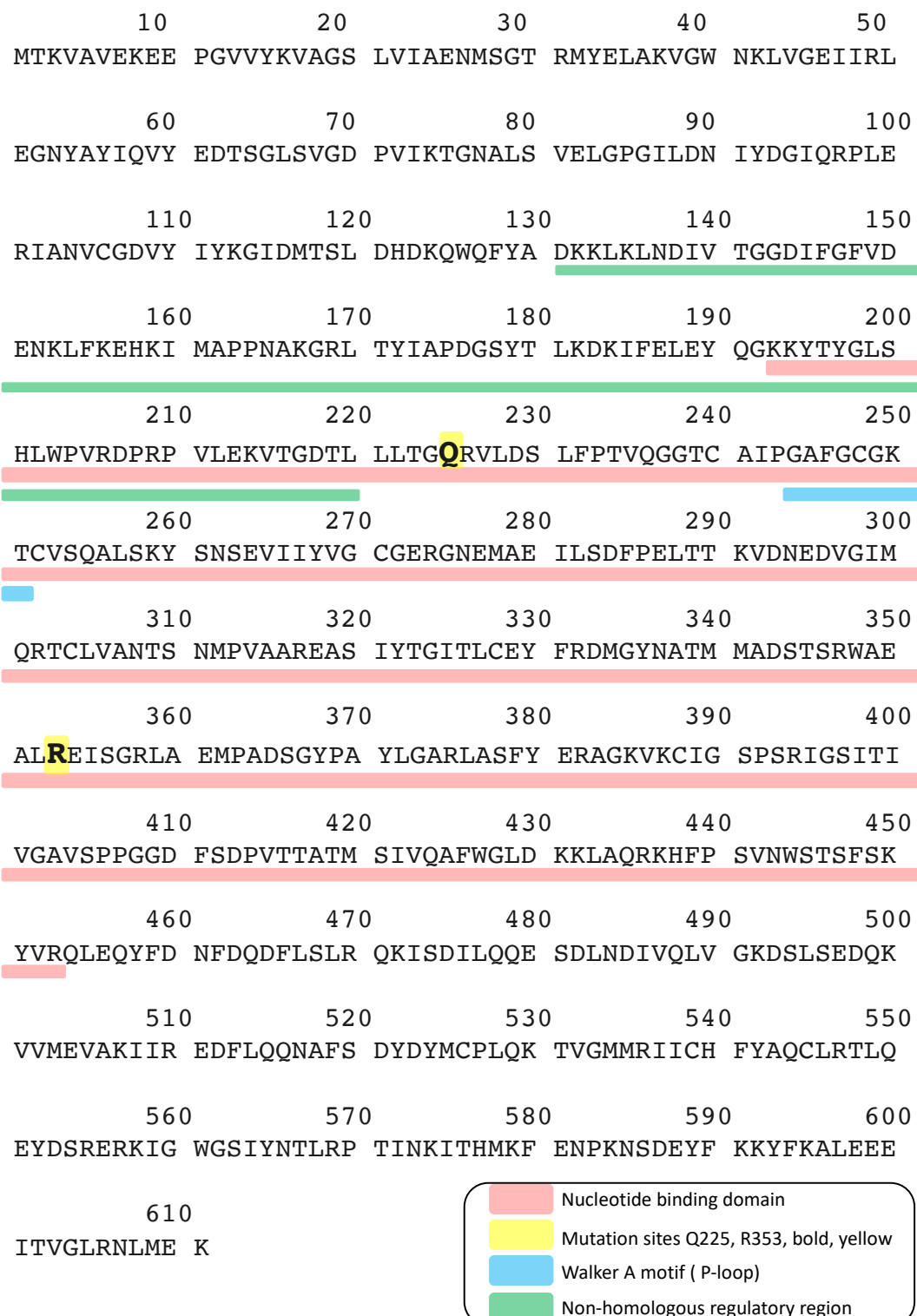
**Supplementary Fig. 5:** Transmission-blocking activity (%TBA) on SMFA. Figure supplementary to Figure 5C. Data are from n=4 biological repeats, mean  $\pm$  S.E. indicated (except for MMV1580853, where only n=3 was performed).



**Supplementary Fig. 6:** Endectocidal activity of 17 compounds with gametocytocidal activity. Compounds were screened at 2  $\mu$ M and mortality of *An. coluzzii* (G3) determined after 4 days, compared to Ivermectin (2  $\mu$ M) as drug control, with DMSO (0.02%) as vehicle control. Data are from n=4 independent biological repeats (except for MMV1580488, MMV000043, MMV68723 which is n=5 and MMV1634399, MMV1006203, MMV1580483 and MMV1174205 which is n=3), mean  $\pm$  S.E.



**Supplementary Fig. 7:** Dose-response of MMV687273 (SQ109, 72 h pressure) against a *PfNCR1*-aptamer inducible knockdown line, where *PfNCR1* expression is controlled by anhydrotetracycline (aTc), with wild type levels of *PfNCR1* retained in presence of aTc (+aTc, 500 nM,  $1.8 \pm 0.08 \mu\text{M}$ ), and *PfNCR1* knock-down induced due to aTc removal (-aTc,  $2.43 \pm 0.15 \mu\text{M}$ ) (unpaired t-test  $p=0.0024$ ). Data are from FACS analysis of parasitemia of acridine orange stained parasites, in triplicates ( $n=3$ ), mean  $\pm$  S.E. 95% confidence intervals on each point indicated as ribbons. Supplementary figure to Figure 7.



**Supplementary Fig. 8:** Sequence of the *P. falciparum* V-type H<sup>+</sup>-ATPase subunit A (PF3D7\_1311900) with domains indicated in coloured bars underneath the sequence as per InterPro analysis <https://www.ebi.ac.uk/interpro/protein/UniProt/Q76NM6/>. The two mutation sites Q225K and R353K are indicated. Supplementary figure to Fig 7.

**Supplementary table 1:** Assay reproducibility for each assay platform (as described in the methods section) as evaluated by Z'-factor parameter according to the equation:  
 $Z' = 1 - [3(\text{SD positive} + \text{SD background}) / (\text{Mean positive} - \text{Mean background})]$ . ABS = asexual blood stages, GC = gametocyte.

Assay platform	Z'-factor
PfNf54 ABS pLDH colorimetric assay	0.63
PfDd2 ABS SYBR Green I fluorescence	0.51
PfNF54 GC ATP bioluminescence	0.864
PfNF54 GC luciferase reporter assay	0.656
PfNF54 GC PrestoBlue fluorescence	0.904
Pb liver assay	0.44
CHO MTT colorimetric	0.64
HepG2 Cell-Titer Glo luminescence	0.52

**Supplementary table 2:** 95% confidence intervals (CI) for IC<sub>50</sub> values of the pan-reactive compounds Birinapant and AZD-0156. Supplementary data to Figure 3.

	MMV1557856 (IC <sub>50</sub> , μM, ± S.E.)	CI	MMV1580483 (IC <sub>50</sub> , μM, ± S.E.)	CI
<b>ABS PfNF54</b>	0.986 ± 0.055	0.8032-1.177	3.998 ± 0.799	2.667-4.161
<b>ABS PfDd2</b>	0.236 ± 0.00	0.17-0.32	0.776 ± 0.079	0.56-1.06
<b>Pf stg IV/V gc</b>	0.135 ± 0.001	0.1149-0.1749	0.236 ± 0.001	0.1983-0.277
<b>Pb liver stage</b>	0.128 ± 0.011	0.0334-0.431	1.055 ± 0.035	0.584-5.47

**Supplementary table 3:** Single nucleotide polymorphisms (SNPs) identified in SQ109-resistant clones compared to the SQ109-sensitive 3D7 parent clone (270 ± 83 nM). SNPs were found in the V-type H+-ATPase subunit A (*Pf3D7\_1311900*) in all four clones, and in the AAA family ATPase (*Pf3D7\_0711000*) for only two clones. Quality refers to the phred-scaled quality score for the alternate base call.

Gene	Chr	SQ109-resistant clone	IC <sub>50</sub> (nM ± S.E.)	Position	Quality	Ref	Alt	Amino acid change
<i>Pf3D7_1311900</i> (V-type H+-ATPase subunit A)	13	SQ1	637 ± 95	508957	6100.46	G	A	R353K
		SQ2	686 ± 123					
		SQ3	632 ± 41		4232.46	C	A	Q225K
		SQ4	572 ± 37					
<i>Pf3D7_0711000</i> (AAA family ATPase)	7	SQ3	632 ± 41	488912	1458.46	G	T	D687N
		SQ4	572 ± 37					